Monte Carlo and Poisson-Boltzmann Study of Electrolyte Exclusion from Charged Cylindrical Micropores

B. Jamnik and V. Vlachy*,†

Contribution from the Department of Chemistry, University of Ljubljana, Ljubljana, Slovenia, and Department of Chemical Engineering and Chemical Sciences Division, Lawrence Berkeley Laboratory, University of California, Berkeley, California 94720. *Received July 8, 1992*

Abstract: The exclusion of model electrolytes from charged cylindrical capillaries is studied using the grand canonical Monte Carlo method and the Poisson-Boltzmann equation. Concentration profiles inside the capillary, Donnan exclusion coefficients, and particle number fluctuations were evaluated for 2:1 (divalent co-ions, monovalent counterions) electrolytes and 1:2 electrolytes (monovalent co-ions, divalent counterions) in the restrictive primitive model approximation for a range of electrolyte concentrations and surface charge densities. The Poisson-Boltzmann equation appears to be a good approximation for 2:1 electrolytes (monovalent counterions) but breaks down completely for 1:2 (divalent counterions) electrolytes in the capillary. The Donnan exclusion coefficient Γ is not an increasing function of the surface charge density, as predicted by the Poisson-Boltzmann equation; rather, it passes through a maximum and decreases with further increase in the surface charge. The same behavior has been observed previously for 2:2 electrolytes. The concentration fluctuations in the capillary, studied for the first time in this work, are much smaller than in the bulk electrolyte solution due to the strong correlations in the electrical double layer. As expected, the concentration fluctuations decrease by increasing the charge on the surface. Finally, a more realistic electrolyte model which fits bulk properties of lithium and cesium chloride solutions very well has also been studied as a function of the surface charge in the capillary. The differences in the electrolyte exclusion between lithium and cesium salt can be explained in view of the short-range forces due to the restructing of water molecules around the ions.

1. Introduction

The problem of electrolyte exclusion from porous media continues to be of interest to many researchers. Following the recent review article,[1] several important papers have been published.[2-8] The methods of statistical mechanics have been used to study the thermodynamics and the interionic correlations of planar slots[2-4] and cylindrical and spherical cavities,[5-7] as well as of water-in-oil micelles.[8] Several recent studies deal with a closely related subject, the evaluation of the force between parallel charged surfaces.[9-11] While the geometry is different, it is evident that the underlying problem in all these studies is a description of the interactions in (or between) electrical double layers, a classical but still challenging topic of the electrochemical science.[12]

The study of the distribution of electrolyte between the porous phase and the bulk solution is fundamental to many chemical, biological, and engineering processes.[1] Usually the concentration of an invading aqueous electrolyte is lower in the porous phase,[13] hence the term "exclusion" of electrolyte. The phenomenon can be understood qualitatively on the basis of interaction between the charge fixed on the inner surfaces and ions of simple electrolyte in the micropore. Due to the charged groups on the internal walls, there is an excess of the counterions next to the surface, while the co-ions are partially excluded from this region. As a result, the co-ion concentration within the capillary is reduced below the bulk value. The Donnan exclusion coefficient, here defined by eq 1, is a convenient measure of this effect. In eq 1, $c_{co\text{-}ion}$ is the

$$\Gamma = \frac{c_{co\text{-}ion} - \langle c_{co\text{-}ion} \rangle}{c_{co\text{-}ion}} \quad (1)$$

concentration of co-ions in the bulk (external) electrolyte and $\langle c_{co\text{-}ion} \rangle$ is the average concentration of co-ions in the micropore.

The major parameters which affect electrolyte exclusion are (i) the concentration and nature of invading electrolyte, (ii) the radius of a micropore, and (iii) the "capacity" of a micropore. The latter quantity is defined as the concentration of (hypothetical) monovalent counterions which neutralize the charge on the inner surface. Experimental results indicate[13-17] that rejection of 1:1 electrolyte increases by increasing the capacity (surface charge) on the capillary. Further, greater rejection is observed for dilute solutions. When charge-asymmetric electrolytes are forced through the membrane, the solutions with divalent co-ions are rejected more strongly than solutions of 1:1 electrolytes. All these results can be understood on the basis of the classical theory of electrical double layers.

The rejection of electrolyte solutions with multivalent counterions has also been studied.[13] In contrast with the results mentioned above, it was found that these systems may exhibit enrichment (not a rejection) of electrolytes in the porous phase. These results cannot be explained by the classical theory of the electrical double layer, and they have been attributed to the specific (non-Coulombic) interactions. A possible explanation for this phenomenon[18,19] is discussed below.

The grand canonical Monte Carlo method has been introduced in the electrical double-layer studies by Valleau and co-workers.[18,19] In the majority of papers, symmetric (1:1 or 2:2) electrolytes are studied in the primitive model approximation. The computer simulation studies of biologically more interesting charge-asymmetric electrolyte or mixtures are less frequent.[11,19,20] In this paper

† Permanent address: Department of Chemistry, University of Ljubljana, Ljubljana, Slovenia.

(1) Vlachy, V.; Haymet, A. D. J. *Aust. J. Chem.* **1990**, *43*, 1961.
(2) Gonzalez-Tovar, E.; Lozada-Cassou, M.; Olivares, W. *J. Chem. Phys.* **1991**, *94*, 2219.
(3) Dubois, M.; Zemb, T.; Belloni, L. *J. Chem. Phys.* **1992**, *96*, 2278.
(4) Feller, S. L.; McQuarrie, D. A. *J. Phys. Chem.* **1992**, *96*, 3454.
(5) Groot, D. E. *J. Chem. Phys.* **1991**, *95*, 9191.
(6) Sloth, P.; Sorenssen, T. S. *J. Chem. Phys.* **1992**, *96*, 549.
(7) Yeomans-Reyna, L.; Gonzalez-Tovar, E.; Lozada-Cassou, M. *Interdisciplinary Conference on Electrified Interfaces*; Book of Abstracts: Asilomar, CA, 1991.
(8) Bratko, D.; Woodward, G. E.; Luzar, A. *J. Chem. Phys.* **1991**, *95*, 5318.
(9) Kjellander, R.; Marčelja, S.; Pashley, R. M.; Quirk, J. P. *J. Chem. Phys.* **1990**, *92*, 4399.
(10) Valleau, J. P.; Ivkov, R.; Torrie, G. M. *J. Chem. Phys.* **1991**, *95*, 520.
(11) Torrie, G. M. *J. Chem. Phys.* **1992**, *96*, 3772.
(12) Blum, L. In *Fluid Interfacial Phenomena*; Croxton, C. A., Ed.; Wiley: New York, 1986; p 391.
(13) Kraus, K. A.; Marcinkowsky, A. E.; Johnson, J. S.; Shor, A. J. *Science* **1966**, *151*, 194.
(14) Marcinkowsky, A. E.; Kraus, K. A.; Phillips, H. O.; Johnson, J. S., Jr., Shor, A. J. *J. Am. Chem. Soc.* **1966**, *88*, 5744.
(15) Jacazio, G.; Probstein, R. F.; Sonin, A. A.; Young, D. *J. Phys. Chem.* **1972**, *76*, 4015.
(16) Westermann-Clark, G. B.; Anderson, J. L. *J. Electrochem. Soc.* **1983**, *130*, 839.
(17) Hijnen, H. J. M.; van Daalen, J.; Smit, J. A. M. *J. Colloid Interface Sci.* **1985**, *107*, 525.
(18) Torrie, G. M.; Valleau, J. P. *J. Chem. Phys.* **1980**, *73*, 5807.
(19) Torrie, G. M.; Valleau, J. P. *J. Phys. Chem.* **1982**, *86*, 3251.

0002-7863/93/1515-660$04.00/0

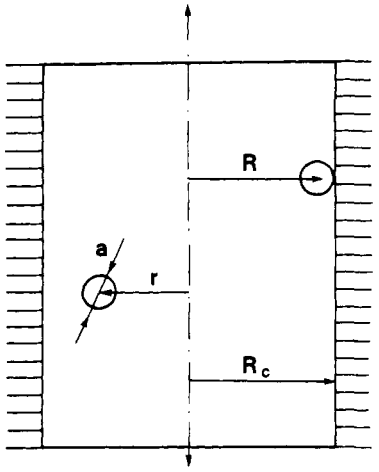

Figure 1. Cross section through the model capillary.

we present one such study. The charge-asymmetric electrolyte in equilibrium with the solution of the same chemical composition contained in a cylindrical micropore is examined. The Donnan exclusion coefficient and ionic distributions were studied for a range of charge densities, electrolyte concentrations, and several values of the diameter of a micropore. The primitive model used in previous calculations depicts the ions as charged hard spheres of equal radii. This approximation is relaxed here. The results are presented for more realistic (nonprimitive) models of aqueous electrolyte solutions. These models yield good agreement with thermodynamic data for isotropic electrolytes[21,22] and permit the study of effects from specific (short-range) interactions on ionic distributions and electrolyte exclusion from a capillary.

2. Methods of Calculation

A. Model Potential. The model used in this study is essentially the same as that described in several previous studies.[1] The porous material is depicted as a collection of equal cylindrical capillaries of radius R_c which do not interact with each other. The capillaries are assumed to be very long, so the end effects can be neglected. The model capillary (Figure 1) is assumed to have the charge uniformly distributed on the inner surface. The parameters of the model can be related to the experimental variables which characterize a given material.[15] The surface charge density is defined as

$$\sigma = \frac{ze_0}{2\pi R_c h} \tag{2}$$

where ze_0 is the charge per length of the micropore h and e_0 is the elementary charge. The interaction potential between the two ions with their centers r_{ij} apart is

$$u_{ij}(r_{ij}) = u_{ij}^*(r_{ij}) + \frac{z_i z_j e_0^2}{4\pi\epsilon_r\epsilon_0 r_{ij}} \tag{3}$$

where ϵ_r is the relative permittivity (the system is treated as dielectric continuum) and $z_i e_0$ (or $z_j e_0$) is the charge on the particular ionic species. In the so-called primitive model, the ions are represented as charged hard spheres of diameter a, so (cf. Figure 1) $R_c = R + a/2$. In this case, $u_{ij}^*(r_{ij})$ reads

$$u_{ij}^*(r_{ij}) = \infty,\ r_{ij} < a \qquad u_{ij}^*(r_{ij}) = 0,\ r_{ij} > a \tag{4}$$

In all the primitive model simulations presented in this paper, a = 0.42 nm.

In part of our calculation, the approximation given by eq 4 is relaxed in favor of a more realistic model of electrolyte solutions:[21,22]

$$u_{ij}^*(r_{ij}) = B_{ij}\left(\frac{(r_i^* + r_j^*)}{r_{ij}}\right)^9 + A_{ij}V_w^{-1}V_m(r_i^* + w, r_j^* + w; r_{ij}) \tag{5}$$

Equation 5 contains two terms: the first one is the repulsive part, where $B_{ij} = 1.804\beta^{-1}$ nm$/(r_i^* + r_j^*)$, and the second term represents the effect of overlapping the hydration shells of ions when r_{ij} is small. As usual, $\beta = (k_B T)^{-1}$, where T is the absolute temperature and k_B is Boltzmann's constant. According to Gurney,[23] the isolated ion is surrounded by a cosphere of water of thickness w (w = 0.276 nm), in which water has different properties than that further away from the ion in the bulk. When two ions come close enough, the sum of their cosphere volumes is reduced by overlap. The mutual (overlap) volume V_m of hydration shells represents the volume of water which must return to its unperturbed (bulk) state. A_{ij} is the change in the molar free energy associated with the process, V_w is the molar volume of the normal solvent, and $V_m(r_i^* + w, r_j^* + w; r_{ij})$ is the mutual volume function, deduced by geometric considerations.[21,23] The model porous material is treated as a dielectric continuum, and the dielectric image effects due to a difference in the permittivity of ions and solvent are ignored here.

B. Grand Canonical Monte Carlo Method. The grand canonical Monte Carlo (GCMC) method has been presented in detail in ref 18. In this kind of simulation, the chemical potential μ is held fixed together with the volume V and temperature T. The first step in the procedure is canonical: a randomly chosen ion is moved into a new random position in the cell. The attempted move is accepted with probability f_{ij}

$$f_{ij} = \min\ [1, \exp(-\beta(U_j - U_i))] \tag{6}$$

where U_i is the configurational energy of state i (old position of the ion) and U_j is the configurational energy of state j. In the next step, a random decision is made to either attempt the insertion or the deletion of a neutral combination of ions $\nu = \nu_+ + \nu_-$, where ν_+ and ν_- are the numbers of positive and negative ions, respectively. The acceptance probabilities for addition and for deletion of ν ions from a micropore are given by eq 7. After the energies

$$f_{ij} = \min\ (1, Y_{ij}),\ \text{for addition}$$
$$f_{ji} = \min\left(1, \frac{1}{Y_{ij}}\right),\ \text{for deletion} \tag{7}$$

U_i and U_j are calculated, the transition probability f_{ij} from the state i with the number of anions N_i^- (and cations N_i^+) to the state j, where $N_j^- = N_i^- + \nu_-$ and $N_j^+ = N_i^+ + \nu_+$) is

$$Y_{ij} = \frac{N_i^+!N_i^-!}{N_j^+!N_j^-!}\exp(B - \beta\ (U_j - U_i)) \tag{8}$$

Parameter B in eq 8 ($B = \beta(\mu - \mu_{ideal}) + \ln\ (N^{\nu_+}{}_+N^{\nu_-}{}_-)$) is related to the excess chemical potential of bulk electrolyte with ionic cations N_+/V and N_-/V which need to be known in advance.

The grand canonical Monte Carlo method has an advantage that, by sampling at constant chemical potential bulk electrolyte phase, is defined unambiguously. Of course, the excess chemical potential of the bulk electrolyte (or B in eq 8) has to be determined in a separate simulation. Although some data are given in the literature,[24,25] we ran our own simulations of the bulk (isotropic) phase for primitive and nonprimitive models.

The GCMC results for the configurational energies, osmotic coefficients, and the mean activity coefficients of bulk LiCl and CsCl aqueous solutions in the nonprimitive model (eq 3), together with the hypernetted-chain (HNC) integral equation results, are reported in Tables I and II. We are not aware of previous simulation based on this model, and it is important to stress the

(20) Zara, J. S.; Nicholson, D.; Parsonage, N. G.; Barber, J. *J. Colloid Interface Sci.* **1989**, *129*, 297.
(21) Ramanathan, P. S.; Friedman, H. L. *J. Chem. Phys.* **1971**, *54*, 1086.
(22) Xu, H.; Friedman, H. L. *J. Solution Chem.* **1990**, *19*, 1155.
(23) Gurney, R. W. *Ionic Processes in Solution*; Dover Publications: New York, 1953.
(24) Valleau, J. P.; Cohen, L. K. *J. Chem. Phys.* **1980**, *72*, 5935.
(25) Vlachy, V.; Ichiye, T.; Haymet, A. D. J. *J. Am. Chem. Soc.* **1991**, *113*, 1077.

Table I. GCMC and HNC Integral Equation Results for a Model LiCl Solution at Several Values of Electrolyte Concentration[a]

c/mol dm^{-3}	$-\beta E_{GCMC}$	$-\beta E_{HNC}$	ϕ_{GCMC}	ϕ_{HNC}	$-\ln \gamma_{\pm,GCMC}$
0.0503	0.211	0.209	0.944	0.945	0.198
0.0754	0.246	0.243	0.938	0.939	0.227
0.1009	0.272	0.269	0.935	0.936	0.248
0.1157	0.286	0.282	0.933	0.935	0.258

[a] $r^*_+ = 0.06$ nm, $r^*_- = 0.181$ nm, $\lambda = 0.713$ nm. The values of Gurney parameters are $A_{--} = A_{++} = 0$ and $A_{+-} = 50$ cal/mol. βE is the reduced configurational energy, ϕ is the osmotic coefficient, and $\gamma_\pm$ is the mean activity coefficient, all evaluated for aqueous solutions at $T = 298$ K. GCMC results are averaged over 5×10^6 configurations. Numerical uncertainties in GCMC results are from 1 to 2%.

Table II. Same as Table I, but for a Model CsCl Solution[a]

c/mol dm^{-3}	$-\beta E_{GCMC}$	$-\beta E_{HNC}$	ϕ_{GCMC}	ϕ_{HNC}	$-\ln \gamma_{\pm,GCMC}$
0.0565	0.242	0.238	0.931	0.923	0.224
0.0768	0.289	0.285	0.920	0.922	0.266
0.1034	0.326	0.323	0.912	0.913	0.298
0.1227	0.350	0.347	0.907	0.909	0.317

[a] $r^*_+ = 0.169$ nm and $r^*_- = 0.181$ nm, $\lambda = 0.713$ nm. The values of Gurney parameters are $A_{--} = 0$, $A_{++} = 100$ cal/mol, and $A_{+-} = -110$ cal/mol.

good agreement between the two types of calculation. The values of Gurney parameters A_{ij} used in this calculation are taken from ref 21. These parameters were obtained by fitting the experimental data for the osmotic coefficients by the hypernetted-chain approximation results for the same quantity.[21]

C. Poisson–Boltzmann Equation. The Poisson–Boltzmann equation for the cylindrical system (see Figure 1) reads[26-33]

$$\frac{1}{r}\frac{d}{dr}\left(r\frac{d\psi}{dr}\right) = -\frac{\rho_e}{\epsilon_0\epsilon_r} \tag{9}$$

$$\rho_e = z_+e_0n_+(0)\, e^{(-z_+e_0\psi\beta)} + z_-e_0n_-(0)\, e^{(-z_-e_0\psi\beta)} \tag{10}$$

where $\psi(r)$ is the mean electrostatic potential at a distance r and $n_i(0)$ is the number concentration of ionic species i at $r = 0$. The appropriate boundary conditions, given by the Gauss Law, are

$$\left(\frac{\partial\psi}{\partial r}\right)_{r=R} = -\frac{\sigma}{\epsilon_0\epsilon_r}$$

$$\left(\frac{\partial\psi}{\partial r}\right)_{r=0} = 0 \tag{11}$$

The Poisson–Boltzmann equation has been solved numerically subject to the boundary conditions using the so-called "shootting method".[34] Once the mean electrostatic potential is known, the ionic distributions and the volume averages needed to determine Donnan exclusion coefficient (eq 1) can readily be calculated.

The Poisson–Boltzmann equation, in its linear or nonlinear version, forms the basis of the classical theory of electrical double layer. The shortcomings of this approximation have been analyzed in many papers, most recently in refs 9–11. The Poisson–Boltzmann equation treats the ions as pointlike charges ignoring their mutual correlations.[35] Computer simulations are free of these approximations and provide data against which the statistical mechanical theories may be tested. One aim of this work is to assess the range of validity of the Poisson–Boltzmann equation for cylindrical micropores.

Table III. GCMC Results for 2:1 (Monovalent Counterions) Electrolytes in Charged Micropores

c_s/mol dm^{-3}	$-\ln \gamma_{\pm,s}$	R/nm	$10^2\,\sigma$/C m^{-2}	Γ[a]
0.0475	0.574	4	3.56	0.66
		4	7.12	0.74
0.0582	0.611	4	3.56	0.60
		4	7.12	0.69
0.0712	0.647	4	3.56	0.54
		4	7.12	0.63
0.1099	0.725	2	0	0.073
		2	1.78	0.56
		2	3.56	0.73
		2	7.12	0.82
		4	0	0.033
		4	1.78	0.29
		4	3.56	0.42
		4	7.12	0.53
		4	10.69	0.55
		4	14.25	0.59

[a] Numerical uncertainties in Γ are estimated to be around 4%.

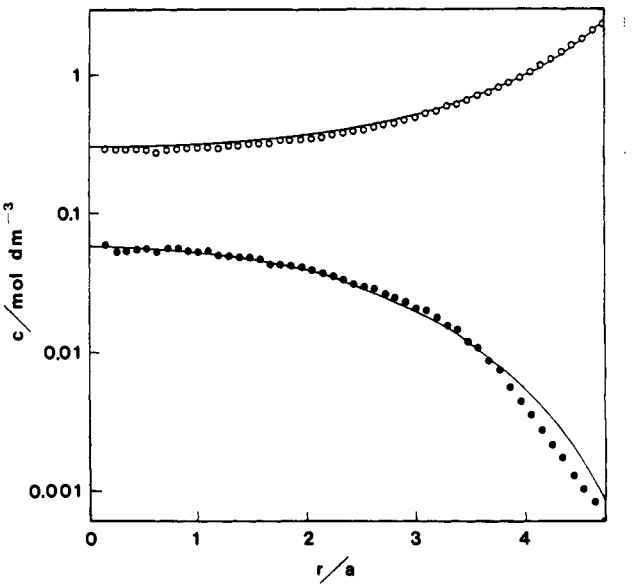

Figure 2. Local concentrations of co-ions (●) and counterions (○) for 2:1 electrolyte inside the micropore, obtained from a GCMC simulation (symbols) and from the Poisson–Boltzmann approximation (solid lines). In this calculation $R = 2$ nm, the concentration of external electrolyte $c_s = 0.1099$ mol/dm^3, $\ln \gamma_{\pm,s} = -0.725$, and surface charge density is $\sigma = 0.0712$ C/m^2.

3. Electrolytes with Monovalent Counterions

In this section we present numerical results for the primitive model of electrolyte (ions of equal size, $a = 0.42$ nm) having divalent co-ions and monovalent counterions (2:1 electrolyte). All calculations presented in Figures 2–4 and in Table III apply to $\lambda_B = \beta e_0^2/(4\pi\epsilon_r\epsilon_0) = 0.714$ nm.

A representative result for ionic distributions inside the micropore is shown in Figure 2. In this calculation, $R = 2$ nm, surface charge density $\sigma = 0.0712$ C/m^2, and the concentration of the bulk (external) electrolyte is $c_s = c_{co\text{-}ion} = 0.1099$ mol/dm^3. As expected, the concentration of counterions next to the charged surface ($r \approx R$), is very high. The Poisson–Boltzmann values, represented by the continuous line, are in a good agreement with the simulation results.

From the predicted ionic distributions, the exclusion coefficients are calculated by using eq 1. Figure 3 shows Γ as a function of

(26) Kobatake, Y. *J. Chem. Phys.* **1958**, *28*, 146.
(27) Dresner, L. *J. Phys. Chem.* **1963**, *67*, 2333.
(28) Rice, C. L.; Whitehead, R. *J. Phys. Chem.* **1965**, *43*, 2111.
(29) Fair, J. C.; Osterle, J. F. *J. Chem. Phys.* **1971**, *54*, 3307.
(30) Levine, S.; Mariott, J. R.; Neale, G.; Epstein, N. *J. Colloid Interface Sci.* **1981**, *82*, 439.
(31) Olivares, W.; Croxton, T.; McQuarrie, D. A. *J. Phys. Chem.* **1980**, *84*, 867.
(32) Dolar, D.; Vlachy, V. *Vestn. Slov. Kem. Drus.* **1981**, *28*, 327.
(33) Vlachy, V.; McQuarrie, D. A. *J. Phys. Chem.* **1986**, *90*, 3248.
(34) Carnahan, B.; Luther, H. A.; Wilkes, J. O. *Applied Numerical Methods*; Wiley: New York, 1969.
(35) Fixman, M. *J. Chem. Phys.* **1979**, *70*, 4995.

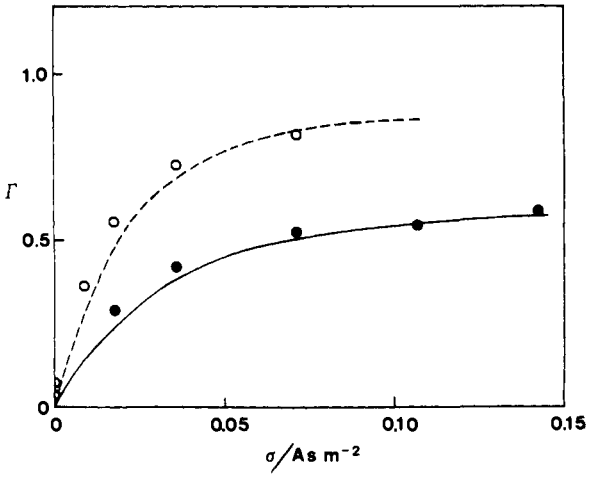

Figure 3. Exclusion parameter Γ as a function of the surface charge density σ for 2:1 electrolyte inside the capillary; c_s = 0.1099 mol/dm^3 and ln $\gamma_{\pm,s}$ = −0.725. Upper curve: R = 2 nm, open circles (○) are GCMC results, and the dashed line represents the Poisson–Boltzmann results. Lower curve: R = 4 nm, solid circles (●) are GCMC results, and the solid line represents the Poisson–Boltzmann results.

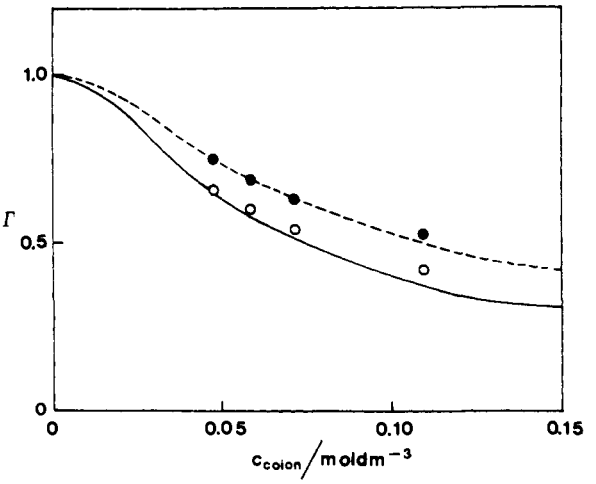

Figure 4. Exclusion parameter Γ for 2:1 electrolytes in micropore (R = 4 nm) as a function of the concentration of co-ions in the external electrolyte, $c_{co\text{-}ion} = c_s$. The dashed line (Poisson–Boltzmann approximation) and the solid circles (●) (GCMC simulations) represent results for σ = 0.0712 C/m^2; the solid line (Poisson–Boltzmann approximation) and the open circles (○) (GCMC simulations) are obtained for σ = 0.0356 C/m^2.

the surface charge density for two different values of R. Both methods predict, in agreement with previous studies on 1:1 electrolytes in micropores,[36,37] that a "saturation" value of Γ will be reached at higher charge densities. Also, smaller micropores are found to be more efficient in excluding electrolytes. In Figure 4, the exclusion coefficient Γ is plotted as a function of the concentration of co-ions, $c_{co\text{-}ion} = c_s$, in the bulk electrolyte. As expected in view of the Coulombic interactions, Γ is increased by decreasing electrolyte concentration. In both cases the agreement between the grand canonical Monte Carlo data and the Poisson–Boltzmann results is good. Smaller discrepancies are observed for very low charge densities, Figure 3, and for higher electrolyte concentrations, Figure 4. Altogether, the Poisson–Boltzmann equation yields reliable results for Donnan exclusion coefficients in solutions with monovalent counterions.

4. Electrolytes with Divalent Counterions

Local concentrations of ions in the solutions of 1:2 electrolytes (monovalent co-ions, divalent counterions) are shown in Figure

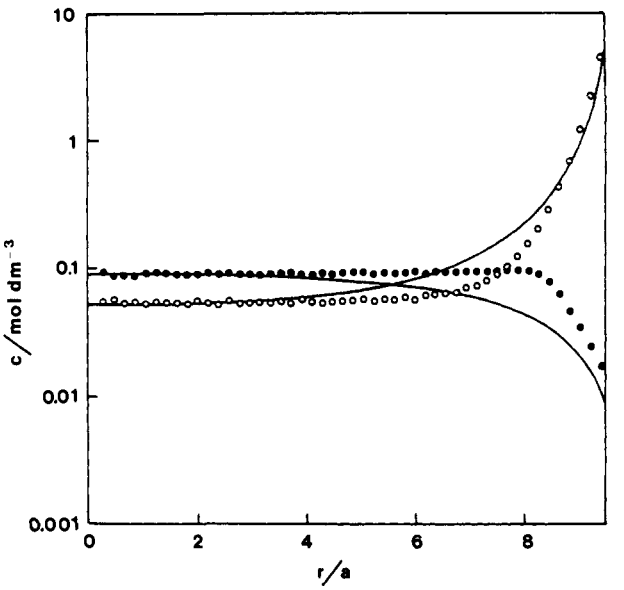

Figure 5. Same as Figure 2, but for 1:2 electrolyte in the capillary. The parameters are R = 4 nm, c_s = 0.0475 mol/dm^3, ln $\gamma_{\pm,s}$ = −0.574, and σ = 0.1425 C/m^2.

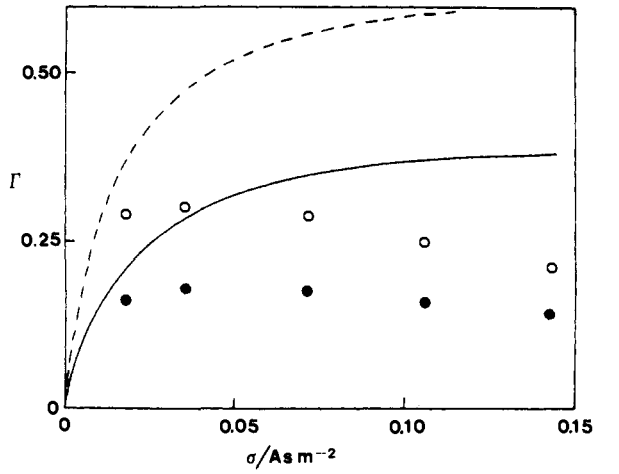

Figure 6. Same as Figure 3, but for 1:2 electrolyte inside the capillary. The parameters are c_s = 0.0475 mol/dm^3, ln $\gamma_{\pm,s}$ = −0.574.

5. The value of R is 4 nm (σ = 0.1425 C/m^2, λ_B = 0.714 nm), and the concentration of bulk electrolyte is c_s = 0.0475 mol/dm^3 ($c_s = 0.5c_{co\text{-}ion}$) for this calculation. In this case, the Poisson–Boltzmann equation (slightly) underestimates the concentration of counterions next to the surface and overestimates the same in the intermediate distances. The distribution of co-ions is much more uniform than that predicted by the Poisson–Boltzmann theory. Also, local concentrations of co-ions obtained by the simulation are higher for all values of r, which significantly affects the predicted exclusion coefficients.

The results for Γ as a function of the surface charge density σ are presented in Figure 6. Monte Carlo exclusion coefficients increase with increasing charge on the surface but eventually reach a maximum and decrease with further increase of σ. Exactly the same behavior has been noticed for aqueous solutions of 2:2 electrolytes in charged micropores.[36,37] The Poisson–Boltzmann theory, in contrast with the simulation results, predicts a monotonic increase of Γ with the surface charge density, which is similar to that in the 2:1 electrolyte case. Also, the exclusion coefficients Γ are actually much lower than predicted by the Poisson–Boltzmann theory; the micropore has a very poor "filtration" ability in the presence of divalent counterions. The concentration dependence of Γ for two different values of the surface charge density is presented in Figure 7. Here, the Poisson–Boltzmann theory yields a qualitatively correct prediction for Γ. All grand canonical

(36) Vlachy, V.; Haymet, A. D. J. *J. Am. Chem. Soc.* **1989**, *111*, 477.
(37) Vlachy, V.; Haymet, A. D. J. *J. Electroanal. Chem.* **1990**, *283*, 77.

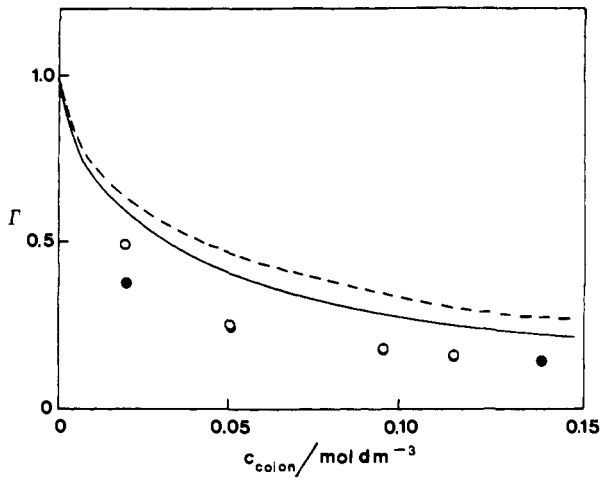

Figure 7. Same as Figure 4, but for 1:2 electrolyte inside the capillary.

Table IV. GCMC Results for 1:2 (Divalent Counterions) Electrolytes in Micropores

c_s/mol dm^{-3}	$-\ln \gamma_{\pm,s}$	R/nm	$10^2\ \sigma$/C m^{-2}	Γ
0.0098	0.328	4	3.56	0.39
		4	7.12	0.375
0.0254	0.469	2	3.56	0.39
		2	7.12	0.37
		4	3.56	0.255
		4	7.12	0.24
0.0475	0.574	2	0	0.077
		2	1.78	0.285
		2	3.56	0.30
		2	7.12	0.285
		2	10.69	0.25
		2	14.25	0.215
		4	0	0.04
		4	1.78	0.16
		4	3.56	0.18
		4	7.12	0.175
		4	10.69	0.16
		4	14.25	0.145
0.0582	0.611	2	3.56	0.28
		2	7.12	0.26
		4	3.56	0.165
		4	7.12	0.16
0.0712	0.647	2	3.56	0.255
		2	7.12	0.24
		4	3.56	0.15
		4	7.12	0.14

Monte Carlo results for Γ presented in this section are collected in Table IV.

5. Concentration Fluctuations

The concentration fluctuations of the electrolyte enclosed in a micropore, defined as

$$S(0) = \frac{\langle N^2 \rangle - \langle N \rangle^2}{\langle N \rangle} \qquad (12)$$

where N is the number of particles in a certain Monte Carlo configuration and $\langle N \rangle$ is its grand canonical average, have not been studied in previous articles. For isotropic electrolyte solutions, $S(0)$ is related to derivaties of the activity coefficients,[25,38] and for one-component liquids, it is proportional to the isothermal compressibility.[38] The ideal gas value of $S(0)$ is 1. In previous papers, grand canonical Monte Carlo and hypernetted-chain (HNC) calculations of $S(0)$ have been presented for symmetric[25] and charge-asymmetric[39] (isotropic) aqueous electrolyte solutions.

(38) Friedman, H. L. *A Course in Statistical Mechanics*; Prentice Hall: Englewood Cliffs, NJ, 1985.
(39) Bešter, M.; Kovačič, B.; Vlachy, V. *Vestn. Slov. Kem. Drus.* **1991**, *38*, 1.

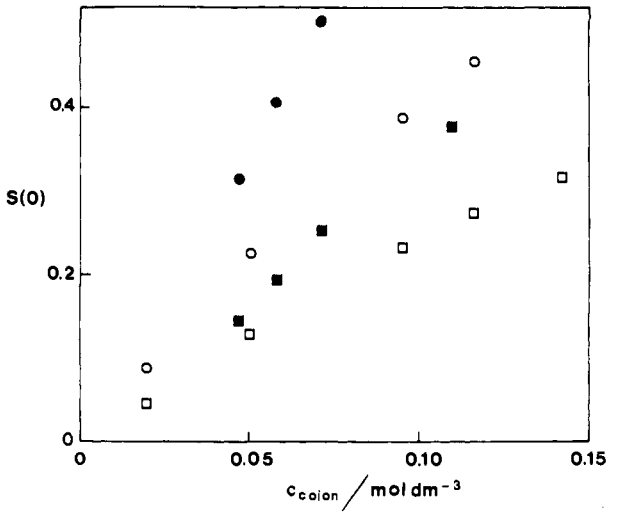

Figure 8. Measure for particle number fluctuations, $S(0)$, inside the cylindrical capillary (R = 4 nm) as a function of $c_{co\text{-}ion}$, obtained from GCMC simulations. (a) 2:1 electrolytes, solid circles (●) represent results for σ = 0.0356 C/m^2, and solid squares (■) are for σ = 0.0712 C/m^2; (b) 1:2 electrolytes, open circles (○) apply to σ = 0.0356 C/m^2 and open squares (□) to σ = 0.0712 C/m^2.

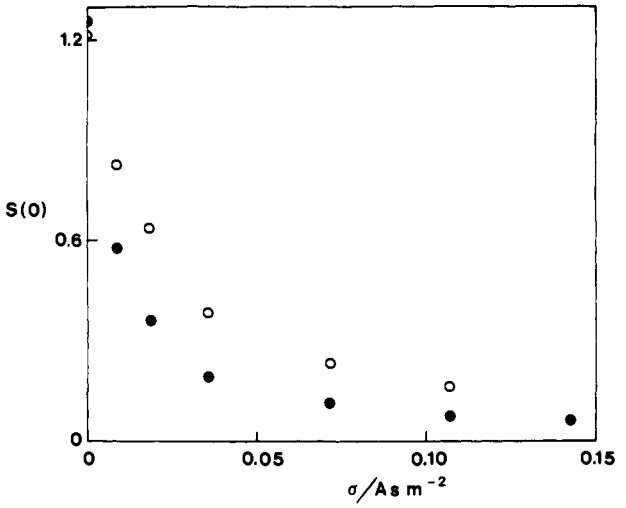

Figure 9. $S(0)$ for 1:2 electrolyte inside the cylindrical capillary as a function of the surface charge density at c_s = 0.0475 mol/dm^3, $\ln \gamma_{\pm,s}$ = −0.574. The open and the solid circles (○, ●) represent the GCMC results for R = 4 nm and for R = 2 nm, respectively.

It is of some interest to examine how the presence of a charged surface affects the concentration fluctuations in electrolyte solutions.

The results for concentration fluctuations are presented in Figures 8 and 9. The value of $S(0)$ in isotropic 2:1 electrolyte is about 1.25 for concentration c_s = 0.0475 mol/dm^3. Due to strong correlations in the charged capillary, the value of $S(0)$ is considerably reduced below its bulk value. The fluctuations are larger for 2:1 electrolytes (compared with 1:2 electrolytes) in the capillary for the same concentration of co-ions and at the same surface charge density σ. Also, as shown in Figure 8, concentration fluctuations increase as the electrolyte concentration for these parameter values is increased. The effect can be understood as a consequence of a stronger electrostatic "screening" of the surface charge by added electrolyte. In Figure 9 we show that the fluctuations are strongly suppressed by an increase in the surface charge density σ. The Poisson–Boltzmann values, however, cannot be ascertained for this quantity. Finally, we note that charge fluctuations are assumed to be 0 for this model of an infinitely long capillary. The situation is different for micellar solutions, where charge fluctuations may play an important role, as described in refs 6 and 8.

Table V. GCMC Results for Γ as a Function of the Surface Charge Density σ^a

$-10^2\sigma$/C m^{-2}	Γ_{LiCl}	Γ_{CsCl}
0.94	0.39	0.385
1.87	0.56	0.54
3.75	0.70	0.67
7.5	0.78	0.735

^{a} For LiCl solution $c_s \approx 0.1009$ mol dm^{-3}, and for CsCl solution $c_s = 0.1034$ mol dm^{-3}; $R_c = 2$ nm, $\lambda = 0.713$ nm. Gurney parameters are given in Tables I and II. Averages are collected over 4×10^6 configurations.

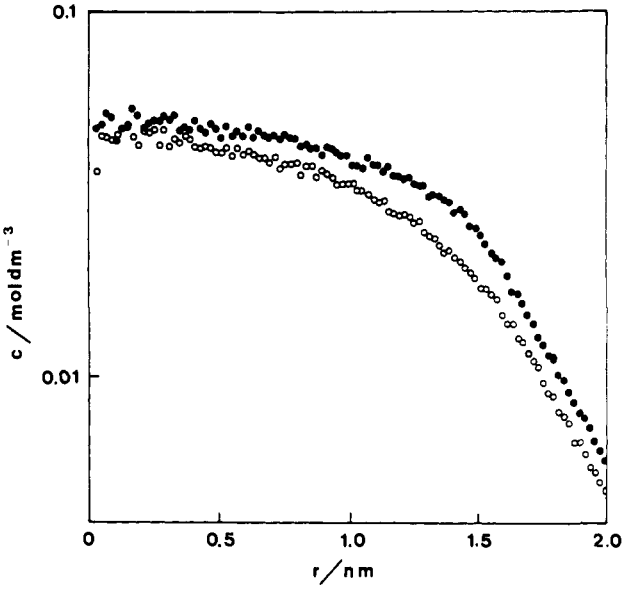

Figure 10. GCMC results for local concentrations of co-ions for LiCl solution (○) and CsCl solution (●) inside the capillary. The results are obtained for $R = 2$ nm and $\sigma = -0.1425$ C/m^2. (a) LiCl, external electrolyte concentration is $c_{LiCl} = 0.1009$ mol/dm^3, ln $\gamma_{\pm,s} = -0.248$; (b) CsCl; external electrolyte concentration is $c_{CsCl} = 0.1034$ mol/dm^3, ln $\gamma_{\pm,s} = -0.298$.

6. Nonprimitive Models

The short-range part of solvent-averaged potential, given by eq 5, is in many aspects a more realistic model for the ion–ion interactions in water than a hard-sphere model.[21-23] In this section we study two different symmetric electrolytes; the parameters in eq 5 are chosen to model aqueous solutions of LiCl and CsCl[21] in charged micropores. The simulation results presented in Table V show that solutions of LiCl are rejected more strongly from charged micropores than CsCl solutions. To illustrate, Figure 10 shows the local concentrations of chlorine ions in LiCl and CsCl solutions through the micropore with $R_c = 2$ nm. Local concentrations of chlorine ions are higher for CsCl solution than for LiCl solution under the same conditions, causing $\Gamma_{LiCl} > \Gamma_{CsCl}$. The results can be explained in view of the interactions between the ions and water molecules: they reflect the strength of the hydration of the particular ionic species. For the solutions with the more strongly hydrated counterion (lithium ion in our case), the exclusion coefficient is higher. The short-range interaction between the lithium and chlorine ion ($A_{+-} = 50$ cal/mol)[21] reflects the fact that the counterion hydration sphere is not easy to penetrate. On the other hand, cesium and chlorine ions ($A_{+-} = -110$ cal/mol) are additionally correlated due to the short-range forces caused by the restructuring of water around the ions. This can make the concentration of chlorine ions inside the micropore higher for CsCl solutions. However, there are other effects of the short-range potential which may not be so easy to elucidate. The (attractive) short-range interaction between the two cesium ions ($A_{++} = -100$ cal/mol) makes an electrical double layer more compact, and one expects (due to stronger screening of the surface charge) a slightly higher rejection in this case. Yet, this effect seems to be less important for the electrolyte exclusion from charged capillaries than the counterion–co-ion correlations described above. The results for uncharged micropores are presented in Table VI.

Table VI. GCMC Results for Uncharged Capillaries^a

LiCl		CsCl	
c/mol dm^{-3}	Γ	c/mol dm^{-3}	Γ
0.0503	0.048	0.0506	0.045
0.0754	0.040	0.0768	0.044
0.1009	0.038	0.1034	0.049
0.1157	0.037	0.1227	0.046

$^a \lambda = 0.713$ nm and $R_c = 2$ nm. Averages are collected over 4×10^6 configurations.

7. Conclusions

The study presented here complements our earlier work on electrolyte exclusion from charged and uncharged cylindrical micropores.[1,36,37] As before, we chose the grand canonical Monte Carlo method to study the distribution of ions inside the capillaries. The results presented above apply to 2:1 aqueous electrolytes (monovalent counterions) and 1:2 electrolytes (divalent counterions) in the restrictive primitive model approximation (ions of equal size) for a range of charge densities σ, bulk electrolyte concentrations c_s, and two different values for the radius of the capillary.

The simulation results are used to test the ability of the Poisson–Boltzmann equation to predict ionic profiles and Donnan exclusion coefficients Γ. The Poisson–Boltzmann approximation has been used to interpret electrokinetic experiments with frequent success.[15-17] Exceptions, however, are studies of solutions with divalent (multivalent) counterions, where experimental results are in a disagreement with the classical Poisson–Boltzmann theory.[13] The grand canonical Monte Carlo results for the local ionic concentrations, exclusion coefficients, and concentration fluctuations presented here indicate strong correlations between divalent counterions and monovalent co-ions in micropores. These correlations may (especially with additional short-range forces between the charged surface and ions) be responsible for the "negative rejection" observed in some cases.[13] This conclusion is not new. A similar behavior has been observed previously in cylindrical systems and 2:2 electrolytes[36,37] and much earlier for planar electrical double layers.[18,19]

In this paper, the first results for the concentration fluctuations inside the charged capillary are presented. As expected, the concentration fluctuations are suppressed due to strong correlations between ions and charged surface. For the model parameters studied here, the concentration fluctuations increase as the concentration of external electrolyte are increased.

Use of the primitive model means the neglect of features like solvation and solvent structure, which may be important at higher concentrations of simple electrolyte. In addition to the restricted primitive model, other electrolyte models were studied. Among electrolytes, lithium chloride and cesium chloride are known to have substantially different osmotic coefficients, and the differences may be attributed to the short-range interactions between various ions. We have shown in section 6 that these (short-range) forces may significantly affect electrolyte exclusion from charged and uncharged capillaries.

The grand canonical Monte Carlo method used in this work is time consuming, and the integral equation theories developed in recent years[12,40-43] (for a review, see refs 12 and 41) represent a more economic alternative. Improvements over the Poisson–Boltzmann approximation (modified Poisson–Boltzmann equation) have also been developed.[44,45] One attractive numerical approach

(40) Lozada-Cassou, M.; Saavedra-Baarera, R.; Henderson, D. *J. Chem. Phys.* **1982**, *72*, 5150.
(41) Carnie, S. L.; Torrie, G. M. *Adv. Chem. Phys.* **1984**, *56*, 141.
(42) Kjellander, R.; Marčelja, S. *J. Phys. Chem.* **1986**, *90*, 1230.
(43) Kjellander, R.; Marčelja, S. *J. Chem. Phys.* **1988**, *88*, 7138.
(44) Outhwaite, C. W.; Bhuiyan, L. *J. Chem. Soc., Faraday Trans. 2* **1983**, *79*, 707.

has recently been suggested by Feller and McQuarrie;[4] their variational solution of the integral equation theory[4] seems to offer both reasonable accuracy and computational simplicity. To our knowledge, with the exception of the preliminary results reported in refs 7 and 33, no numerical data based on the solution of the integral equation theories for the cylindrical micropores have been published so far.

(45) Outhwaite, C. W. *J. Chem. Soc., Faraday Trans. 2* **1986**, *82*, 789.

Acknowledgment. The support of the Research Community of Slovenia is gratefully acknowledged. The authors thank Dr. Dirk Stigter and Stephen Lambert for critical reading of the manuscript.

Aminoalkyl and Alkylaminium Free Radicals and Related Species: Structures, Thermodynamic Properties, Reduction Potentials, and Aqueous Free Energies

David A. Armstrong,* Arvi Rauk,* and Dake Yu

Contribution from the Department of Chemistry, The University of Calgary, Calgary, Alberta, Canada T2N 1N4. *Received July 14, 1992*

Abstract: The structures of $H_2NCH_2^+$, $H_2NCH_2^{\bullet}$, H_2NCH_3, $H_2NCH_3^{\bullet+}$, $H_3NCH_2^{\bullet+}$, $(CH_3)_2NCH_2^+$, $(CH_3)_2NCH_2^{\bullet}$, $(CH_3)_3N$, and $(CH_3)_3N^{\bullet+}$ were optimized at the HF/6-31G* and MP2/6-31+G* levels, and the frequencies were calculated at the HF/6-31G* level. For $H_2NCH_2^+$, $H_2NCH_2^{\bullet}$, H_2NCH_3, $H_2NCH_3^{\bullet+}$, and $H_3NCH_2^{\bullet+}$ the total energies were evaluated at the G2 level and those of $(CH_3)_2NCH_2^+$, $(CH_3)_2NCH_2^{\bullet}$, $(CH_3)_3N$, and $(CH_3)_3N^{\bullet+}$ at the level of MP2/6-31+G*+ZPE. Where comparisons were possible, heats of formation from these results agreed well with recent literature data. On the basis of the structural information from the ab initio calculations and an analysis of the solution free energies of the parent compounds, solution free energies were calculated for the radicals studied by the G2 procedure and several others for which reliable heats of formation were available. These data were used to obtain values of $\Delta_f G°(aq)$ and reduction potentials for the $R^1R^2NCR^3H^{\bullet}$ radicals in reaction 2: $R^1R^2NCR^3H^{\bullet} + e^- + H^+ \rightarrow R^1R^2NCR^3H_2$. The values of $\Delta_f G°(aq)$ for several ionic species were obtained from literature data and used to calculate values of $E°_{(6)}$ for reaction 6: $R^1R^2NCR^3H_2^{\bullet+} + e^- \rightarrow R^1R^2NCR^3H_2$. Estimates of $E°_{(1)}$ for reaction 1, $R^1R^2NCR^3H^+ + e^- \rightarrow R^1R^2NCR^3H^{\bullet}$, were also obtained. These confirmed the strong reducing character of the α-amino radicals. Existing experimental data on aqueous solutions are discussed in the light of the present results.

1. Introduction

Apart from their intrinsic interest in organic chemistry, α-carbon-centered and nitrogen-centered free radicals of amines are of practical importance in several areas. For example, they have been postulated as intermediates in the photochemistry of nitrosamines[1] and in the reaction mechanisms of some amine oxidases,[2,3] and they are frequently used in biological chemistry as reducing agents.[4] The same radicals are probably also involved when amines are used as sacrificial hydrogen donors in redox systems activated by solar energy.[5] Typical redox reactions which have been proposed[6] are written below for a generalized radical, $R^1R^2NCR^3H^{\bullet}$, with R^1, R^2, and R^3 representing organic groups or H atoms. The radical II is seen to be the intermediate redox form between the iminium I and the amine III. The second

$$\underset{\text{I}}{R^1R^2NCR^3H^+} + e^- \rightarrow \underset{\text{II}}{R^1R^2NCR^3H^{\bullet}} \qquad E°_{(1)} \qquad (1)$$

$$\underset{\text{II}}{R^1R^2NCR^3H^{\bullet}} + e^- + H^+ \rightarrow \underset{\text{III}}{R^1R^2NCR^3H_2} \qquad E°_{(2)} \qquad (2)$$

reaction probably occurs sequentially, with prior protonation followed by rapid electron transfer. Experimental work[6,7] has shown that II is protonated to form the N-centered radical IV:

$$\underset{\text{II}}{R^1R^2NCR^3H^{\bullet}} + H^+ \rightarrow \underset{\text{IV}}{R^1R^2NCR^3H_2^{\bullet+}} \qquad \Delta G°_{(3)} \qquad (3)$$

rather than the C-centered radical V

$$\underset{\text{II}}{R^1R^2NCR^3H^{\bullet}} + H^+ \rightarrow \underset{\text{V}}{R^1R^2NHCR^3H^{\bullet+}} \qquad \Delta G°_{(4)} \qquad (4)$$

In the above, and in subsequent equations for reactions, we indicate the quantities of interest which will be evaluated. For example, $E°_{(1)}$ is the reduction potential in aqueous solution for reaction 1 and $\Delta G°_{(3)}$ is the free energy change for reaction 3.

Scheme I

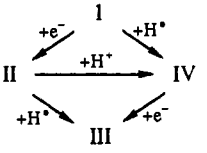

There are two other redox reactions that must be considered:

$$\underset{\text{I}}{R^1R^2NCR^3H^+} + e^- + H^+ \rightarrow \underset{\text{IV}}{R^1R^2NCR^3H_2^{\bullet+}} \qquad E°_{(5)} \qquad (5)$$

and

$$\underset{\text{IV}}{R^1R^2NCR^3H_2^{\bullet+}} + e^- \rightarrow \underset{\text{III}}{R^1R^2NCR^3H_2} \qquad E°_{(6)} \qquad (6)$$

* The authors to whom correspondence should be addressed.

(1) Chow, Y. L. *Acc. Chem. Res.* **1973**, *6*, 354.
(2) Singer, T. P., Van Korff, R. W., Murphy, D. L., Eds. *Monamine Oxidase: Structure, Function, and Altered Functions*; Academic Press: New York, 1979.
(3) (a) Silverman, R. B.; Hoffman, S. J. *J. Am. Chem. Soc.* **1980**, *102*, 884. (b) Simpson, J. T.; Krantz, A.; Lewis, F. D.; Kokel, B. *J. Am. Chem. Soc.* **1982**, *104*, 7155.
(4) See, for example: Armstrong, J. S.; Hemmerich, P.; Traber, R. *Photochem. Photobiol.* **1982**, *35*, 747 and references therein.
(5) Hoffman, M. Z. *J. Phys. Chem.* **1988**, *92*, 3458.
(6) Chow, Y. L.; Danen, W. C.; Nelsen, S. F.; Rosenblatt, D. H. *Chem. Rev.* **1978**, *78*, 243.
(7) Das, S.; von Sonntag, C. *Z. Naturforsch.* **1986**, *41b*, 505. Das, S.; Schuchmann, M. N.; Schuchmann, H.-P.; von Sonntag, C. *Chem. Ber.* **1987**, *120*, 319.

0002-7863/93/1515-666$04.00/0